

YIELD OF SECONDARY ELECTRON EMISSION FROM CERAMIC MATERIALS OF HALL THRUSTER WITH SEGMENTED ELECTRODES

A. Dunaevsky, Y. Raitses, and N. J. Fisch

Plasma Physics Laboratory, Princeton University, P.O.Box 451, Princeton, NJ 09543, US

The discharge parameters in the Hall thrusters depend strongly on the yield of secondary electron emission from the channel walls. Comparative measurements of the yield of secondary electron emission at low energies of primary electrons were performed for several dielectric materials used in Hall thrusters with segmented electrodes. The measurements showed that in low energy region the actual energetic dependencies of the yield of secondary electron emission could differ from fits which are usually used in theoretical models. For instance, at low energies of primary electrons, energetic dependencies for different dielectric materials should cross each other. The origin of the observed difference could be in surface properties, while at higher energies, where fits based on power law are relevant, properties of the material bulk play determinative role.

Introduction

Secondary electron emission (SEE) plays an important role in physics of Hall thrusters. Higher secondary electron emission from ceramic walls in so-called stationary plasma thrusters (SPT) might result in a lower electron temperature and a longer acceleration region, in comparison to thrusters with anode layer (TAL) with metal channel walls [1, 2]. The performance of the SPT differs for different materials of the channel walls [3]. Segmented electrodes made of a material with different secondary emission properties have been shown to affect the potential distribution in the SPT channel, which in turn may be a cause of the observed 20% reduction of the plasma plume divergence [4, 5, 6]. The use of materials with different SEE to affect both the potential profile in an SPC and thereby the efficiency has been explored also theoretically [7, 8]. Thus, it is of great importance to describe precisely SEE in the transition region between a wall and neutral plasma.

Flow of secondary electrons from the wall was introduced into model of the plasma sheath by Hobbs and Wesson [9]. Assuming the Boltzmann distribution for plasma electrons, they expressed the potential drop on the sheath in presence of secondary electron emission. This model assumes the Bohm velocity at the sheath edge and did not consider plasma-sheath

transition. In modern models of SPT [10, 11], the actual radial velocity at the sheath edge is calculated from presheath models in presence of the SEE flux.

Calculations showed that the potential drops in the sheath – presheath and, as a result, electron losses on the channel walls depend strongly on the yield of SEE [11]. The distribution of the electron temperature along the channel is also affected by SEE [10]. Therefore, relevance of calculations depends strongly on correctness of the SEE data.

At present, there is no systematic measurements of $\sigma(E_p)$ at $10 < E_p \leq 100$ eV for the most of modern ceramics and dielectric materials. Existing theories of SEE [12, 13] are able to predict the behavior of $\sigma(E_p)$ only at $E_p > 80-100$ eV. Therefore, the yield of SEE in SPT models is usually determined from various fits. Power fit

$$\sigma(E_p) \approx \left(\frac{E_p}{E_1} \right)^\alpha \quad (1)$$

was used by Ahedo [8] and by Jolivet and Roussel [14]. Here E_1 corresponds to energy at which $\sigma=1$. In this model, therefore, the values of $\sigma(E_p)$ for one material will remain higher (or lower) than correspondent values for another material in whole range of E_p . The same nature of $\sigma(E_p)$ is conjectured by the most of authors who deal with interactions of low temperature plasmas with dielectric walls.

Such an assumption, however, should become incorrect at low energies of primary electrons. Moreover, the yield of electron induced SEE from dielectrics depends on temperature [15], angle of incident electrons [16], surface roughness [17], bounded surface charge [18, 19], and other effects, which become important at low energies. The behavior of $\sigma(E_p)$ for different materials at $E_p \leq 100$ eV should be more complicated, as it follows from our measurement presented below.

Experimental setup

Direct measurements of the yield of SEE at low energies of primary electrons are complicated because of the charging of the sample surface. The surface will acquire a positive charge if the flux of secondary electrons is higher than primary flux, and negative in the opposite case. The electric field of the surface charge changes the energy of primary electrons. The uncertainty in measurements induced by surface charging should reach several times [20]. In order to minimize the effect of the surface charging, primary electron beam can be modulated by short pulses [21, 15]. The amplitude of the primary current and the duration of the current pulse should be short in order to minimize the influence of the surface charging. From the charge

conservation law, the total current in the sample circuit can be expressed as a sum of the surface leakage current, I_c , and the displacement current:

$$I = C \frac{dV_s}{dt} + I_c \quad (2)$$

where C is the sample capacitance. Neglecting by the surface leakage current, the surface voltage V_s will increase linearly along with the current pulse of the primary electron beam:

$$V_s = \frac{I_p d}{\epsilon \epsilon_0 \pi r^2} t \quad (3)$$

Here d and ϵ are the sample thickness and the dielectric constant, and r is the radius of the beam focal spot. At low energies of primary electrons, the total SEE yield is less than unity. Therefore, one should consider the maximal charging current $I \sim I_p$. Assuming $\epsilon \sim 2$, $d = 0.3$ mm, $I_p = 50$ nA, and $r = 0.5$ mm, the surface voltage should reach $V_s \sim 1$ V in $t \sim 1$ μ s. Thus, at $E_p = 10$ eV the pulse duration of the primary electron beam is limited by $\tau < 1$ μ s by the desired uncertainty of the energy of primary electrons $\leq 10\%$.

One can see that V_s can be decreased by the increase of the focal spot radius and by the decrease of the sample thickness. The decrease of d will also lead to the increase of the time constant of the measuring circuit, RC , which is required to be higher than τ , and to decrease the influence of parasitic capacitances.

Our experimental setup is represented schematically in Fig. 1. The primary electron beam was generated by an electron gun ELG-2 produced by Kimball Physics, Inc. The range of electron energies was 6 – 1000 eV; the maximal beam current was 10 mA. The minimal diameter of the beam focal spot was 1 mm. The duration of the pulse can be set down to 100 ns, which was set by an external 6040 pulse generator produced by Berkley Nucleonic Corp.

Samples were mounted on a sample holder made of boron nitride. The parasitic capacitance between the rear sample electrode and ground was minimized to < 1.5 pF. The sample holder was attached to the high vacuum sample heater produced by HeatWave Corp. The temperature of the samples was monitored by K-type thermocouple mounted into the sample holder. The sample holder was mounted on a rotating stage, together with a Faraday cup for measurement of the primary current, I_p (see Fig.1).

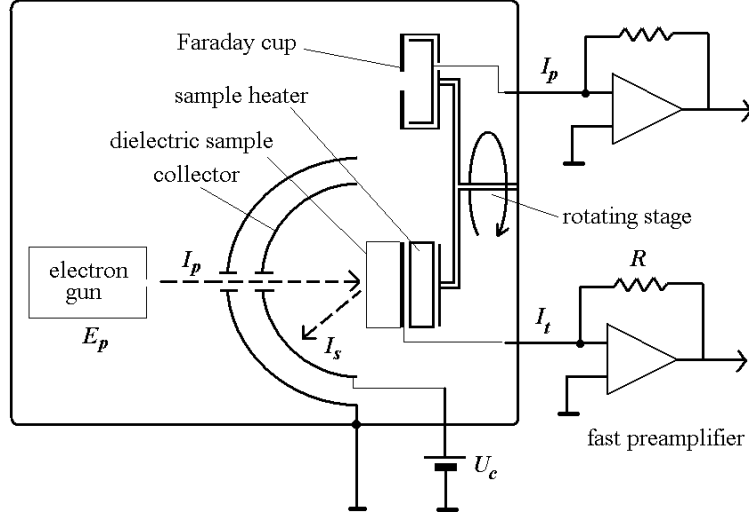


Figure 1. Experimental setup.

The signals from the sample and from the collector were amplified by direct coupled fast amplifiers with the input resistance of 200 k Ω and the bandwidth limit of 10 MHz. Amplified signals were recorded by the Tektronix digitizing oscilloscope. The total yield of SEE was determined as:

$$\sigma = \frac{I_s}{I_p} = \frac{I_p - I_t}{I_p} \quad (4)$$

where I_t is the displacement current measured in the sample circuit. The potential of the collector, U_c , was chosen in the range of 10-15 V depending on the material and E_p .

After each shot, the vacuum chamber was opened and the surface of the samples was cleaned by a volatile conducting solvent with the following heating at 150-200 $^\circ$ C in vacuum of about 10^{-7} Torr. This procedure does not provide complete removal of the surface charge, which is accumulated inside the material on the depth of several monolayers. However, repetitive measurements at the same primary energy showed the deviation of the SEE yield less than 5-10%.

Results and discussion

The results of our measurements of the total yield of SEE at energies lower than 100 eV are presented in Fig. 2 for two materials, boron nitride and quartz, together with the results of other authors [23, 24]. One can see that the present measurements of $\sigma(E_p)$ from SiO₂ appear in good agreement with the results reported by Dionne [23]. Some difference in SEE yield from

boron nitride was observed between our present measurements and the measurements performed by of Bugeat and Koppel [24]. Our results appear closer to measurements by Dawson [25] who found for boron nitride $E_I \approx 50$ eV. In our measurements, we used samples made of boron nitride grade HP produced by Saint Gobain Corp.

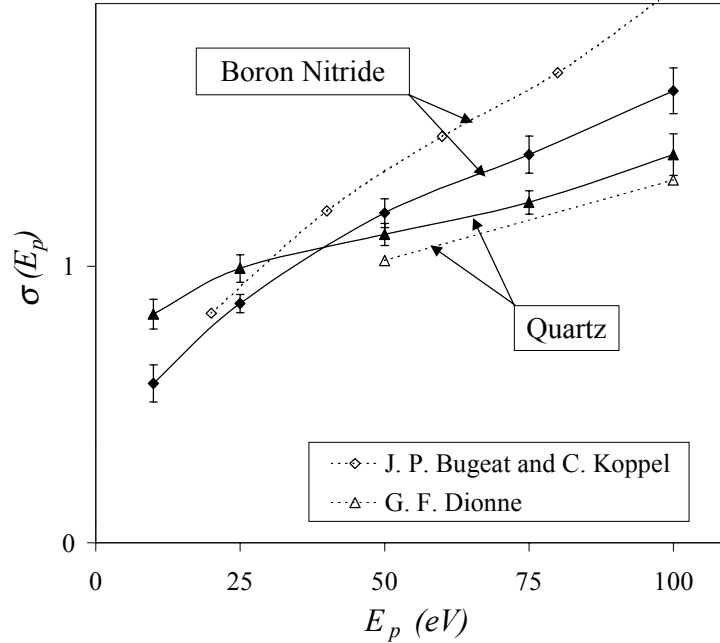


Figure 2. Total yield of the secondary electron emission from boron nitride and quartz at $E_p < 100$ eV. Dashed lines represent the previous measurements of SEE yield made by Dionne [23] and Bugeat and Koppel [24] for quartz and for boron nitride, respectively.

The obtained results show that the dependencies of $\sigma(E_p)$ should cross each other at low energies of primary electrons. The same crossing was observed also for pair boron nitride – macor in the same energy range. The origin of the crossing should be in surface properties. Indeed, primary electrons with higher energies can penetrate deeper in the material [13]. Thus, the absorption of primary and the production secondary electrons occurs in the material bulk and could depend more on bulk material properties and less on surface properties. Primary particles with energies of a few tens of eV could involve in the production of secondary particles only thin surface layer of the material. Material surface can have structure different from the bulk material, it can contain impurities and absorbed gases, can be contaminated, etc. The sample temperature can change the slope of $\sigma(E_p)$ in the low energy range [15]. The role of the surface roughness is growing with the decrease of the primary energy as well [17]. Thus, the yield of SEE should differ from fits based on parameters like σ_{max} measured at higher primary energies. However, the

actual surface conditions could also lead to substantial difference between measurements in the low energy range.

The measured behavior of $\sigma(E_p)$ at low energies of primary electrons suggests a possible deviation from the power fit. The flow of secondary electrons from boron nitride wall should be lower than, for instance, from macor wall at low plasma electron temperatures but higher at higher temperatures. The observed dependence seems closer to the linear approximation suggested by Morozov in [26]. However, taking into account the dependence of the yield of SEE on the surface conditions and the temperature, the specific type of approximation for each material should be checked experimentally.

Acknowledgments

This work was supported by the New Jersey Commission of Science and Technology, and by the DOE under contract DE-AC02-76-CH03073.

References

- [1] V. V. Zhurin, R. H. Kaufman, and R. S. Robinson, *Plasma Sources Sci. Technol.* **8**, R1 (1999).
- [2] E. Y. Choueiri, *Phys. Plasmas* **8**, 5025 (2001).
- [3] Y. Raitses, J. Ashkenazy, G. Appelbaum, and M. Gualman, *25th International Conference on Electric Propulsion, Cleveland, OH*, IEPC 97-056 (1997).
- [4] Y. Raitses, L. A. Dorf, A. A. Litvak, and N. J. Fisch, *J. Appl. Phys.* **88**, 1263 (2000).
- [5] N.J. Fisch, Y. Raitses, L. A. Dorf and A. A. Litvak, *J. Appl. Phys.* **89**, 2040 (2001).
- [6] Y. Raitses, M. Keidar, D. Staack, and N. J. Fisch, *J. Appl. Phys.* **92**, 4906 (2002).
- [7] A. Fruchtman, N.J. Fisch, and Y. Raitses, *Phys. Plasmas* **8**, 1048 (2001).
- [8] A. Fruchtman and N.J. Fisch, *Phys. Plasmas* **8**, 56 (2001).
- [9] G. D. Hobbs and J. A. Wesson, *Plasma Physics* **9**, 85 (1967).
- [10] M. Keidar, I. D. Boyd, and I. I. Beilis, *Phys. Plasmas* **8**, 5315 (2001).
- [11] E. Ahedo, *Phys. Plasmas* **9**, 4340 (2002).
- [12] H. Seiler, *J. Appl. Phys.* **54**, R1 (1983).
- [13] K. Kanaya, S. Ono, and F. Ishigaki, *J. Phys. D: Appl. Phys.* **11**, 2425 (1978).
- [14] L. Jolivet and J.-F. Roussel, *3rd Int. Conf. on Spacecraft Prop. Cannes, ESA/CNES* (2000).
- [15] J. B. Johnson, *Phys. Rev.* **73**, 1058 (1948).
- [16] A. Shih and C. Hor, *IEEE Trans. on Electron Devices* **40**, 824 (1993).
- [17] Y. C. Yong, J. T. L. Thong, and J. C. H. Phang, *J. Appl. Phys.* **84**, 4543 (1998).
- [18] T. Sato, S. Kobayashi, S. Michizono, and Y. Saito, *Appl. Surface Sci.* **144-145**, 324 (1999).

- [19] L. L. Hatfield and E. R. Adamson, in *Proc. of IEEE Int. Conf. on Electrical Insulation and Dielectric Phenomena, Arlington, TX, October 23-26*, 256, (1994).
- [20] J. Cazaux, *J. Appl. Phys.* **85**, 1137 (1999).
- [21] H. L. Heydt, *Rev. Sci. Instrum.* **21**, 639 (1950).
- [22] H. von Seggern, *IEEE Trans. Nucl. Sci.* **NS-32**, 1503 (1985).
- [23] G. F. Dionne, *J. Appl. Phys.* **46**, 3347 (1975).
- [24] J. P. Bugeat, and C. Koppel, *23th International Conference on Electric Propulsion, IEPC 95-35* (1995).
- [25] P. H. Dawson, *J. Appl. Phys.* **37**, 3644 (1966).
- [26] A. I. Morozov, *Sov. Journal of Plasma Phys.* **17**, 824 (1991).